

Effects of Geometrical Symmetry on the Vortex Nucleation and Penetration in Mesoscopic Superconductors

Xing-Hua Hu¹, An-Chun Ji², Xiang-Gang Qiu^{1*} and Wu-Ming Liu¹
¹*Beijing National Laboratory for Condensed Matter Physics,
 Institute of Physics, Chinese Academy of Sciences, Beijing 100190, China and*
²*Center of Theoretical Physics, Department of Physics,
 Capital Normal University, Beijing 100048, China*

(Dated: December 13, 2018)

We investigate how the geometrical symmetry affects the penetration and arrangement of vortices in mesoscopic superconductors using self-consistent Bogoliubov-de Gennes equations. We find that the entrance of the vortex happens when the current density at the hot spots reaches the depairing current density. Through determining the spatial distribution of hot spots, the geometrical symmetry of the superconducting sample influences the nucleation and entrance of vortices. Our results propose one possible experimental approach to control and manipulate the quantum states of mesoscopic superconductors with their topological geometries, and they can be easily generalized to the confined superfluids and Bose-Einstein condensates.

PACS numbers: 74.78.Na, 74.25.Ha, 74.81.-g

The advances in modern nanotechnology and the development of quantum computing have opened many new perspectives for research on mesoscopic superconductors [1]. One fascinating aspect in mesoscopic superconductivity is the novel physics associated with vortices, which has been a subject of great experimental [2–10] and theoretical [11–14] interest in the past decades. In the mesoscopic superconductors, vortices are quantized and confined by the sample geometry, so they can exhibit many unique phenomena compared with conventional bulk superconductors. For example, when the sample is mesoscopic, the giant vortex can form, and there may exhibit the exotic paramagnetic Meissner effect [12]. Further, it is shown that the symmetry of the sample geometry can dramatically affect the properties of the mesoscopic system [9]. Recent experiment has also reported the symmetry-induced antivortices formation [7], which is a unique character of a mesoscopic superconductor. However, how the geometrical symmetry of sample can control the vortex state is hitherto not well understood.

In this Letter, we explore the effect of symmetry on the vortex nucleation and entrance in the mesoscopic superconductor far below the critical temperature. We develop an effective numerical method to generally solve the Bogoliubov-de Gennes (BdG) equations [15], which is based on the finite element method (FEM) [16, 17]. Compared with the conventional Ginzburg-Landau (GL) theory [18], the BdG equations work well in wider temperature region, and can give the spectrum of excitations for spatially inhomogeneous superconductor self-consistently, supposed the few fundamental material parameters are given. Several groups have successfully used the BdG equations to study the single vortex line [19–22].

Here, we solve the BdG equations self-consistently, and obtain the vortex pattern and the current density in mesoscopic superconductors with arbitrary and com-

plicated geometries. Our results show that the current distribution and the penetration of vortices are determined by the symmetry of the sample geometry, and the entrance of the vortex happens only when the current density at the hot spots (i.e. the spots with maximum current density) reaches the depairing current density. These facts reveal unambiguously that the geometrical symmetry of the superconducting sample influences the nucleation and entrance of vortices, *through determining the spatial distribution of hot spots*. These results provide a practicable route to manipulate the quantum states of a mesoscopic superconductors in future applications.

We start with the BdG equations for the quasiparticle wave functions $u_n(\mathbf{r})$ and $v_n(\mathbf{r})$ in the presence of a magnetic field

$$\begin{aligned} \left[\frac{1}{2m} \left(\frac{\hbar}{i} \nabla - \frac{e\mathbf{A}}{c} \right)^2 - \mu \right] u_n(\mathbf{r}) + \Delta(\mathbf{r})v_n(\mathbf{r}) &= E_n u_n(\mathbf{r}), \\ \left[\frac{-1}{2m} \left(\frac{\hbar}{i} \nabla + \frac{e\mathbf{A}}{c} \right)^2 + \mu \right] v_n(\mathbf{r}) + \Delta^*(\mathbf{r})u_n(\mathbf{r}) &= E_n v_n(\mathbf{r}), \end{aligned} \quad (1)$$

where E_n is the n -th energy eigenvalue, $\Delta(\mathbf{r})$ the pair potential, $\mathbf{A}(\mathbf{r})$ the vector potential and μ the chemical potential.

The pair potential $\Delta(\mathbf{r})$ is determined self-consistently by

$$\Delta(\mathbf{r}) = g \sum_{|E_n| \leq E_c}^n u_n(\mathbf{r})v_n^*(\mathbf{r})(1 - 2f(E_n)), \quad (2)$$

where g is the interaction constant, $f(E)$ the Fermi distribution function and E_c the cutoff energy which is related by the BCS relation via the transition temperature T_c and the superconducting energy gap Δ_0 .

The vector potential $\mathbf{A}(\mathbf{r})$ is related to the current distribution $\mathbf{j}(\mathbf{r})$ by Maxwell's equation

$$\nabla \times \nabla \times \mathbf{A}(\mathbf{r}) = \frac{4\pi}{c} \mathbf{j}(\mathbf{r}), \quad (3)$$

where the current distribution [15, 21] is given by

$$\mathbf{j}(\mathbf{r}) = \frac{e\hbar}{2mi} \sum_n \left[f(E_n) u_n^*(\mathbf{r}) (\nabla - \frac{ie}{\hbar c} \mathbf{A}(\mathbf{r})) u_n(\mathbf{r}) + (1 - f(E_n)) v_n(\mathbf{r}) (\nabla - \frac{ie}{\hbar c} \mathbf{A}(\mathbf{r})) v_n^*(\mathbf{r}) - H.c. \right]. \quad (4)$$

The chemical potential μ is determined by the particle number conservation imposed on this system [20]

$$N = 2 \int \sum_n \{ f(E_n) |u_n(\mathbf{r})|^2 + (1 - 2f(E_n)) |v_n(\mathbf{r})|^2 \}, \quad (5)$$

where N is the total number of particles.

The boundary conditions for the above equations are given by

$$\mathbf{n} \cdot \left(\frac{\hbar}{i} \nabla - \frac{e}{c} \mathbf{A} \right) u_n = 0, \quad \mathbf{n} \cdot \left(\frac{\hbar}{i} \nabla + \frac{e}{c} \mathbf{A} \right) v_n = 0, \quad (6)$$

where we consider two dimensional superconducting samples placed in the (x, y) plane, which are immersed in insulating medium in the presence of a perpendicular uniform magnetic field along z direction. \mathbf{n} is the normal vector of the boundary.

We numerically solve Eqs.(1)-(6) self-consistently, based on finite elements method [16, 17]. All input parameters used in the calculation are microscopic parameters which can in principle be obtained from band structure calculations [21]. These parameters consist of the cutoff energy E_c , the coupling constant g and $k_F \xi_0$ [19], where k_F (v_F) is the Fermi wave number (velocity) and $\xi_0 = \hbar v_F / \Delta_0$ the coherence length.

In this paper, we consider the system at the temperature $T = 0.1T_c$ and choose $E_c = 5\Delta_0$ and $k_F \xi_0 = 2$. To conveniently compare our results with the experiment, other parameters are chosen so as to make the Ginzburg-Landau parameter κ to be a specified value, where $\kappa = 0.96\lambda_L(0)/\xi_0$ [15] and $\lambda_L(0)$ is the London penetration depth. We consider a square superconductor with the length of a side $a = 5\xi_0$ and $\kappa = 20$. The sample is first cooled down into the superconducting state, and then we slowly increase the magnetic field and solve the BdG equations at each field, mimicing the zero field cooling measurements [2, 3]. The global magnetization M can be calculated as $M = 1/(2S) \int_S \mathbf{r} \times \mathbf{j} dx dy$, where S is the sample area. In the frame of BdG theory, the

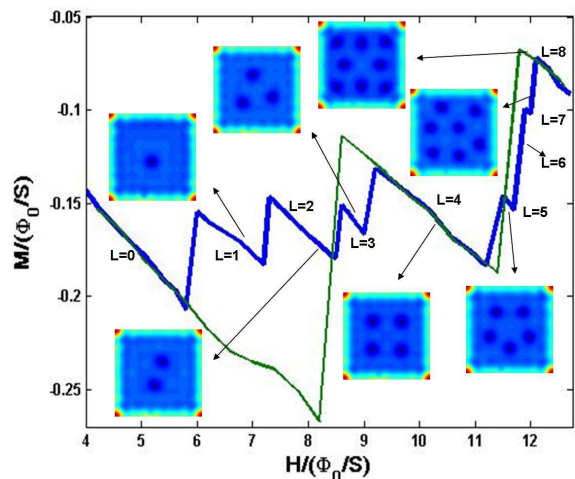


FIG. 1: (Color online) Magnetization (M) versus the external magnetic field (H) for a superconducting square sample without (thin line) and with (thick line) one defect. The vorticity L are labeled near the branches. For the sample with one defect, the corresponding vortex pattern at each L is given as the contour plots on the insets.

free energy \mathcal{F} of the system is given [23] by

$$\begin{aligned} \mathcal{F} = & 2 \sum_n E_n f(E_n) - 2 \sum_n E_n \int d^3\mathbf{r} |v_n(\mathbf{r})|^2 \\ & - 2k_B T \sum_n \{ f(E_n) \ln f(E_n) + [1 - f(E_n)] \ln [1 - f(E_n)] \} \\ & + \int d^3\mathbf{r} \frac{|\Delta(\mathbf{r})|^2}{g} + \int d^3\mathbf{r} \frac{|\mathbf{H}(\mathbf{r}) - \mathbf{H}_0|^2}{8\pi}, \end{aligned}$$

where k_B is the Boltzmann constant, \mathbf{H}_0 the external magnetic field and $\mathbf{H}(\mathbf{r})$ the spatial dependent magnetic field inside the sample.

Shown in Fig. 1 is the \mathbf{H}_0 dependent magnetization of the square sample. We can see that the magnetization shows a zigzag-like pattern. Each descending branch of the zigzag can be described by a fluxoid number L (vorticity), which determines how many times the phase of pair potential $\Delta(\mathbf{r})$ change by 2π along the sample's circumference. Here L is just the number of vortices. Sweeping the magnetic field continuously, the magnetization evolves along one of the fluxoid curves until it reaches its end and jumps to the next curve, belonging to another fluxoid state.

In a perfect square sample with four-fold symmetry, we find that vortices enter the sample in unit of 4 with $L = 4n$ ($n = 0, 1, 2, \dots$), and they replicate the geometrical symmetry of the sample, see Fig. 1. Note that the vortices enter the sample as 4 individual single quantum vortices rather than a giant vortex, which is in agreement with the previous works [17, 24]. However, if we reduce the sample size or increase the temperature, the vortices merge into one giant vortex. Further, upon the entrance of vortices, the magnetization displays a sudden jump to

the next branch. And correspondingly the free energy of the system drops discontinuously. This is consistent with the fact that the superconductor under consideration here is a type II one, which characterizes a negative surface energy [14]. Besides, we also study samples with other geometries, such as rectangle which has a two-fold symmetry, and disk which is rotation-invariant. In the case of rectangle, our results show that the vortices penetrate the sample in pair, just as expected. While for a disk, the Meissner state persists until $H > 12\Phi_0/S$, indicating that the critical field for vortex penetration is much larger than other geometry, which has been reported in experiment [6]. Thus, the above results suggest that the geometrical symmetry of sample determines how the vortices enter the sample.

When the symmetry of sample is broken by placing one defect on the sample boundary, the situation is dramatically changed. As an example, we consider the square sample with one sharp defect located at $2/5$ of the length at the bottom edge, which mimics the practical experiment realized in ref. [6]. While in the perfect sample, the vortices enter in unit of 4, in the sample with one defect, the vortices enter one by one. Furthermore, from the vortex pattern (see the inset in Fig. 1), we can see that when the number of vortices inside the sample becomes large, the increased interaction between vortices dominates over the influence of the boundary, which makes the triangular lattice a favorable arrangement. The system free energy follows the same trend as in the perfect square, once a vortex enters the sample, the free energy of system makes a discontinuous drop to a lower energy level. This confirms the determining influence of the sample symmetry on the vortex penetration and arrangement.

Now we address how the geometrical symmetry determines the vortex entrance and which intrinsic material parameter controls the nucleation and entrance of the vortices. We calculated the current density inside the samples $\mathbf{j}(\mathbf{r})$. The current distributions at several representative fields are shown in Fig. 2. It is evident that the current distribution conforms to the geometrical symmetry. In the perfect square sample (Fig. 2, contour plot I), the current density distribution has a four-fold symmetry, forming 4 equivalent hot spots where the current density is the highest. Upon increasing the magnetic field, the current density at the hot spots increases monotonously until it reaches a critical current j_c simultaneously. Further increasing the magnetic field results in the nucleation of vortices at the hot spots, and at the same time the current density drops to a magnitude much smaller than j_c . For the sample with one defect (Fig. 2, contour plot II), the process is the same except that there is only one hot spot, due to the addition of the defect. Consequently, the change of current distribution leads to the large deviation of vortex entrance behavior. We notice that the critical current density for the vor-

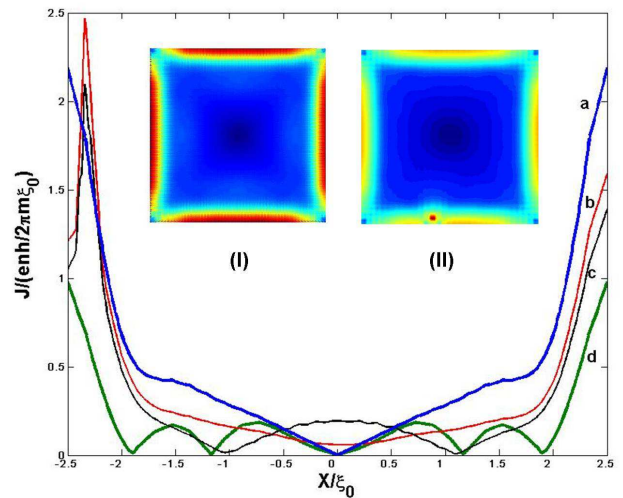


FIG. 2: (Color online) The spatial dependent current density of the sample. The insets (I) and (II) are the contour plots of the magnitude of current density for the sample without and with a defect, respectively. The lines correspond to the intersecting line of the current density in (I) and (II). The solid line **a** and **d** are for the perfect sample under the magnetic field $H = 8.3\Phi_0/S$ (**a**, before the vortex entrance) and $H = 8.4\Phi_0/S$ (**d**, after the vortex entrance); the thin line **b** and **c** are the intersecting line across the defect, under the magnetic field $H = 5.6\Phi_0/S$ (**c**, before the vortex entrance) and $H = 5.8\Phi_0/S$ (**b**, after the vortex entrance);

tex nucleation $j_c \sim 2.5en\hbar/m\xi_0$ is roughly equal to the depairing current density derived from London theory, $J_c = cH_c/4\pi\lambda = 2.56en\hbar/m\xi_0$. These facts suggest that in the mesoscopic superconductors, the intrinsic material parameter that determines the nucleation of vortices is the depairing current density.

We further consider the cases where there are two defects on the sample boundary. When the defects distribute symmetrically, for example, the two defects are at the middle positions of opposite edges, the sample has two fold symmetry and two equivalent hot spots are formed around the two defects. Thus the vortices enter the sample in pair through the defects, as shown in Fig. 3a. On the contrary, if the defects are not equivalent, there is a difference between the maximum current density at the defects. As a result, the vortex penetrates the sample one by one, and the vortex nucleates first at the defect with higher maximum current density.

Therefore, our results support such a scenario for the vortex nucleation and entrance in the mesoscopic superconductor: When an external magnetic field is applied, before the penetration of vortices, the magnetic field is screened out by the circulating current, resulting in a Meissner state. The spatial distribution of current is determined by the symmetry of the sample geometry and the distribution of defects. The points where the magnitude of current are maximum will form hot spots. As the magnetic field increases, the current density at the hot

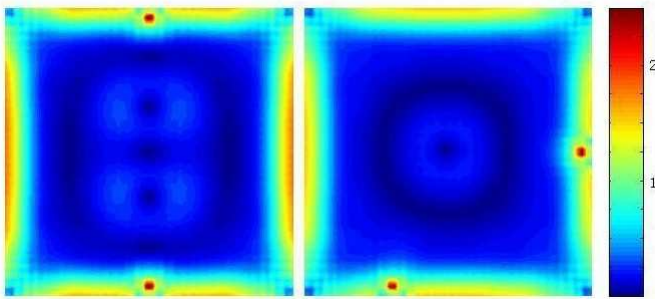


FIG. 3: (Color online) The contour plots of the magnitude of current density of the sample with two defects at the magnetic field $H = 6.2\Phi_0/S$. At this magnetic field, two vortices (left) and one vortex (right) has penetrated into the sample. The left is the sample with two defects arranged symmetrically at the middle of up and bottom edges, while in the right, two defects are not equivalent.

spots increases correspondingly. Once the current density at the hot spots reach the depairing current density, vortices will nucleate at the hot spots and enter the superconductor. Accompanying the entrance of vortex, the system magnetization and free energy have one discontinuous drop and the system jumps to the next quantum state through a first order phase transition. Thus the geometric symmetry of the sample influences the spatial distribution of the hot spots, resulting in different vortex entrance behaviors. The influence of geometrical symmetry is a general property of the confined vortex system, thus this scenario can be easily generalized to the confined superfluids and Bose-Einstein condensates.

In conclusion, by developing an effective numerical method to solve the BdG equations self-consistently, the effect of the geometrical symmetry on vortex penetration in mesoscopic superconductors and its mechanism are studied quantitatively. We demonstrated that, the condition of the nucleation of vortex is that the current density at hot spots reaches the depairing current density. The geometrical symmetry influences the vortex nucleation and entrance through determining the spatial distribution of hot spots. The entrance of vortices leads to one first-order transition between the quantum states with different number of vortices. Our results suggest that by modifying the topological factors such as geometrical symmetry and defects etc., it is possible to control the entrance and location of the vortices, and thus the quantum states. In practical experiment, one can control the quantum states of a mesoscopic superconductor by tuning the applied magnetic field or current density. This opens up an applicable way to manipulate the quantum states in mesoscopic superconductors, which is crucial for nano-devices based on mesoscopic superconductors.

The authors would like to thank fruitful discus-

sions with Jiang-Ping Hu. This work was supported by NSFC under grants Nos. 10974241, 10874235, 10934010, 60978019, the NKBRFC under grants Nos. 2009CB929100, 2009CB930701 and 2010CB922904.

* Electronic address: xgqiu@aphy.iphy.ac.cn

- [1] K. Kadowaki, *Sci. Technol. Adv. Mater.* **6**, 589 (2005).
- [2] T. Cren, D. Fokin, F. Debontridder, V. Dubost, and D. Roditchev, *Phys. Rev. Lett.* **102**, 127005 (2009).
- [3] T. Nishio *et al.*, *Phys. Rev. Lett.* **101**, 167001 (2008).
- [4] I. V. Grigorieva, W. Escoffier, J. Richardson, L. Y. Vinnikov, S. Dubonos, and V. Oboznov, *Phys. Rev. Lett.* **96**, 077005 (2006).
- [5] S. B. Field, S. S. James, J. Barentine, V. Metlushko, G. Crabtree, H. Shtrikman, B. Ilic, and S. R. J. Brueck, *Phys. Rev. Lett.* **88**, 067003 (2002).
- [6] A. K. Geim, S. V. Dubonos, I. V. Grigorieva, K. S. Novoselov, F. M. Peeters, and V. A. Schweigert, *Nature* **407**, 55 (2000).
- [7] L. F. Chibotaru, A. Ceulemans, V. Bruyndoncx, and V. V. Moshchalkov, *Nature* **408**, 833 (2000).
- [8] A. K. Geim, S. V. Dubonos, J. J. Palacios, I. V. Grigorieva, M. Henini, and J. J. Schermer, *Phys. Rev. Lett.* **85**, 1528 (2000).
- [9] V. V. Moshchalkov, L. Gielen, C. Strunk, R. Jonckheere, X. Qiu, C. V. Haesendonck, and Y. Bruynseraede, *Nature* **373**, 319(1995).
- [10] H. F. Hess, R. B. Robinson, and J. V. Waszczak, *Phys. Rev. Lett.* **64**, 2711 (1990).
- [11] E. H. Brandt, *Phys. Rev. B* **59**, 3369 (1999).
- [12] V. V. Moshchalkov, X. G. Qiu, and V. Bruyndoncx, *Phys. Rev. B* **55**, 11793 (1997).
- [13] B. J. Baelus, A. Kanda, N. Shimizu, K. Tadano, Y. Ootuka, K. Kadowaki, and F. M. Peeters, *Phys. Rev. B* **73**, 024514 (2006).
- [14] J. Bonca and V. V. Kabanov, *Phys. Rev. B* **65**, 012509 (2001).
- [15] P. G. Gennes, *Superconductivity of Metals and Alloys*(Addison-Wesley, Reading, MA,1989).
- [16] O. C. Zienkiewicz, R. L. Taylor, and J. Z. Zhu, *The Finite Element Method Its Basis and Fundamentals 6th ed.* (Elsevier, Singapore, 2008).
- [17] H. Suematsu, M. Machida, T. Koyama, T. Ishida, and M. Kato, *Physica C* **412**, 548 (2004).
- [18] M. Tinkham, *Introduction to Superconductivity* (McGraw-Hill, Inc. USA, 1996).
- [19] N. Hayashi, T. Isoshima, M. Ichioka, and K. Machida, *Phys. Rev. Lett.* **80**, 2921 (1998).
- [20] M. Kato and K. Maki, *Prog. Theor. Phys.* **103**, 867 (2000).
- [21] F. Gygi and M. Schlüter, *Phys. Rev. B* **43**, 7609 (1991).
- [22] A. S. Melnikov, D. A. Ryzhov, and M. A. Silaev, *Phys. Rev. B* **79**, 134521 (2009).
- [23] I. Kosztin, S. Kos, M. Stone, and A. J. Leggett, *Phys. Rev. B* **58**, 9365 (1998).
- [24] S. Kim, J. Burkhardt, M. Gunzburger, J. Peterson, and C. R. Hu, *Phys. Rev. B* **76**, 024509 (2007).